Publishing Excellence
Inspiring Progress
ARISTON PUBLICATIONS

Energy & Environment Advances

ISSN: 3066-5728 https://aristonpubs.com/energy-environment-advances https://doi.org/10.69626/eea.2024.0015

RESEARCH ARTICLE

Study on the Numerical Modeling of CdTe/CdS/SnO_2 Based Thin Film Solar Cells Using SCAPS–1D

Anju Rani [1], Mrinal Dutta [2], Chander Shekhar [1], Ayana Bhaduri [1,*]

ABSTRACT: In response to changes in material or design, a suitable simulator can be used to predict the novel solar cell's performance. Employing one dimensional Solar Cell Capacitance Simulator (SCAPS-1D) software, this work analyses cadmium telluride (CdTe) solar cell's fundamental parameters & performance. The solar cell used for this work is comprised of CdTe(p)-CdS(n)-$SnO_2(n^+)$; where CdTe, SnO_2, and CdS act as absorber layer, window layer and buffer layer respectively. The work primarily focuses on 1) layer thickness optimization for various layers, 2) the impact of the CdS layer's electron affinity, and 3) the impact of a highly doped (p^+) thin layer of CdTe acting as the PV device's back surface field [1]. The band gap and thickness of the layers are kept constant during simulation at their ideal or predetermined levels. The employed CdTe(p), CdS(n) and $SnO_2(n^+)$ band gaps are 1.5eV, 2.4eV, and 3.6eV, respectively, with corresponding thicknesses of 2.0 µm, 25 nm, and 0.5 µm. The solar cell's efficiency dropped from 19.24% to 18.63% as the electron affinity of the CdS layer rose from 3.75eV to 4.2 eV. The addition of a 0.1 µm thick p^+ rear surface layer increased the efficiency of the solar cell to 21.96%. The optimized absorber, buffer and window layer thicknesses are 4 µm, 15 nm and 0.2µm correspondingly. At an electron affinity of 3.75 eV for the CdS layer, the highest output cell efficiency metrics obtained are J_{SC}=25.141mA/cm^2, V_{OC}=1.0538V, FF%=88.16 % and η%=23.36%.

Keywords: SCAPS-1D, Thin-film Solar cell, CdTe, CdS, SnO_2, Electron Affinity, Back Surface Field.

Received: 18 January 2024; Revised: 16 February 2024; Accepted: 18 February 2024; Published Online: 01 March 2024

1. INTRODUCTION

Fossil fuel has been utilized for many years to satisfy the rising energy needs of the world's consumption-oriented economies, but its supply is limited. Therefore, to meet the energy requirements, only renewable energy sources will be able to supply the greatly increased energy demands sustainably [1, 2]. Amongst the sustainable renewable energy sources, solar energy is inexhaustible, environment-friendly, and cost-effective: hence one of the viable candidates in this situation [3]. Introducing improved solar cell designs, new materials, optimized growth conditions, and cost-effective manufacturing can produce more affordable and efficient devices, enabling solar photovoltaic energy systems to reach their full potential. The key component in solar photovoltaic research is the efficiency/cost ratio [4].

There are few solar cell PV technologies with over 20% efficiency namely c-Si, CIGS, GaAs, CdTe and Perovskite solar cells [5]. However each of the technologies has its challenges, for instance, the limited supply of feedstock material for c-Si technology, the high cost of material processing and device manufacturing, and the incapacity for monolithic interconnections are the main concerns [6]. However, the principal disadvantages of thin film-based solar cells such as CdTe, CIGS, CIS, GaAs are the toxicity of Cd, the scarcity of Te, Ga and In, the difficulty in establishing stoichiometric ratio, and the occurrence of secondary phases and the manufacturing cost of the GaAs and CIGS solar cells [7-8]. Commercial usage of perovskite solar cells is hindered by two main issues: the use of the hazardous substance lead (Pb) and organic cations, which are hygroscopic and volatile

[1] Department of Physics, Amity School of Applied Sciences, Amity University Haryana, Gurugram, 122413, India
[2] National Institute of Solar Energy, Gurugram, Haryana 122003, India

* Author to whom correspondence should be addressed: ayana.bhaduri@gmail.com (A. Bhaduri)

© Ariston Publications 2024. All rights reserved.

and can cause thermal and chemical instability, reducing their lifespan [9].

A reliable, economical, and promising contender for photovoltaic (PV) energy generation in this respect is cadmium telluride (CdTe)/cadmium sulphide (CdS) based thin film solar cells. The advantage of CdTe as a direct band gap material is that it has a greater absorption coefficient than silicon and is easier to manufacture devices. It may be deposited on glass as thin layer films at low temperatures, with a few micrometers thickness [10-13]. Making minor adjustments to one parameter at a time has traditionally and experimentally been a laborious process for creating new solar cells. Instead of highly expensive, time-consuming, and sophisticated experiments, extensive simulation software are now more readily available which are cost effective, versatile and faster [12–14] in generating the output of the solar cells. This work aims to analyze a CdTe-based solar cell's photovoltaic performance employing SCAPS-1D.

2. METHODOLOGY

The performance of solar cell structures has been simulated in the current work employing 'Solar Cell Capacitance Simulator 1-Dimensional' (SCAPS-1D), a computer simulation programme [13-15]. Figure 1 exhibits the SCAPS-1D action panel with all the parameters as used for the present study. In addition, Figure 2 demonstrates schematic illustration of SCAPS-1D panel structure based solar cell.

2.1. Mathematical model employed in SCAPS-1D simulation software

By employing the continuity equation for electrons and holes to solve the following Poisson equation, performance characteristics such as the current density-voltage (J-V) curve, power conversion efficiency, energy band gap, etc. may be determined [2].

$$\frac{d}{dz}\left[-\epsilon(z)\frac{d\emptyset}{dz}\right] = q[p(z) - n(z) + N_D^+(z) - N_A^-(z) + p_t(z) - n_t(z)] \quad (1)$$

$$\frac{dp_n}{dt} = G_p - \frac{p_n - p_{n0}}{\tau_p} + p_n\mu_p\frac{d\varepsilon}{dz} + \mu_p\varepsilon\frac{dp_n}{dz} + D_p\frac{d^2p_n}{dz^2} \quad (2)$$

$$\frac{dn_p}{dt} = G_n - \frac{n_p - n_{p0}}{\tau_n} + n_p\mu_n\frac{d\varepsilon}{dz} + \mu_n\varepsilon\frac{dn_p}{dz} + D_n\frac{d^2n_p}{dz^2} \quad (3)$$

Where G, D, τ_n, τ_p, q, Φ,ξ, μ_n, μ_p, n(z), p(z), $n_t(z)$,$p_t(z)$, $N^-_A(z)$and $N^+_D(z)$ are the rate of generation, coefficient of diffusion, lifetime of an electron, lifetime of a hole, electronic charge, electric potential, electric field, e-mobility, hole-mobility, free electron concentration, free hole concentration, trapped e-concentration, trapped hole-concentration, ionized acceptor concentration and ionized donor concentration, correspondingly. The direction is denoted by Z.

The optical properties, such as recombination, reflection, and absorption, along with the light irradiation spectrum, are the main determinants of the short circuit current density (J_{sc}). The J_{sc} of the solar cell could be computed by equation (4) given below [16, 17]:

$$J_{sc} = q\sum T(\lambda)\frac{\emptyset_i(\lambda_i)}{hv_i}\eta(\lambda_i)\Delta\lambda_i \quad (4)$$

Where, q is electronic charge, $\Delta\lambda_i$ is the distance between two consecutive wavelength values, $\emptyset_i$ stands for the spectral power density, and T(λ) stands for the optical transmission.

The open-circuit voltage, V_{oc}, is the voltage that the solar cell experiences when there is no net current flowing through it. It may be expressed as stated in equation (5) as:

$$V_{oc} = \frac{nkT}{q}\ln\left(\frac{J_{sc}}{J_o} + 1\right) \quad (5)$$

Equation (6) may be used to express the fill factor percent, FF%, which is solar cell's maximum power:

$$FF\% = \frac{V_{OC} - \ln(V_{OC} + 0.72)}{V_{OC} + 1} \quad (6)$$

AM 1.5 G, the standard solar cell spectrum (direct as well as diffused) is used as incident illumination for estimating the J-V characteristics of solar cells.

The energy conversion efficiency η %, of solar cell can be expressed by relation (7) as:

$$\eta\% = \frac{V_{OC}\times J_{SC}\times FF\%}{P_{in}} \quad (7)$$

The suggested input power i.e.,P_{in}, of the sun is 1000 W/m^2.

The solar cells used in this study are constructed with a CdTe(p)-CdS(n)-SnO_2(n+) configuration, where cadmium telluride (CdTe) serves as the absorber layer, cadmium sulfide (CdS) as the window layer, and tin dioxide (SnO_2) as the buffer layer. This investigation focuses on the impact of altering the electron affinity of the CdS layer and incorporating a highly doped thin CdTe (p+) layer as a back surface field (BSF) to enhance the photovoltaic (PV) device's performance. To maintain consistency, key characteristics such as the band gaps and layer thicknesses are kept constant during the simulation. The band gaps for CdTe(p), CdS(n), and SnO_2(n+) are 1.5 eV, 2.4 eV, and 3.6 eV, respectively. The respective thicknesses of the layers are 2.0 µm, 25 nm, and 0.5 µm. This study aims to provide insights into optimizing layer properties to improve solar cell efficiency and performance.

Table 1 shows a list of the relevant optical and electrical parameters that were employed in the simulations for further consideration. The majority of the simulation's input parameters have been mostly gathered from relevant theories and literature [17-18].

 © Ariston Publications 2024. All rights reserved

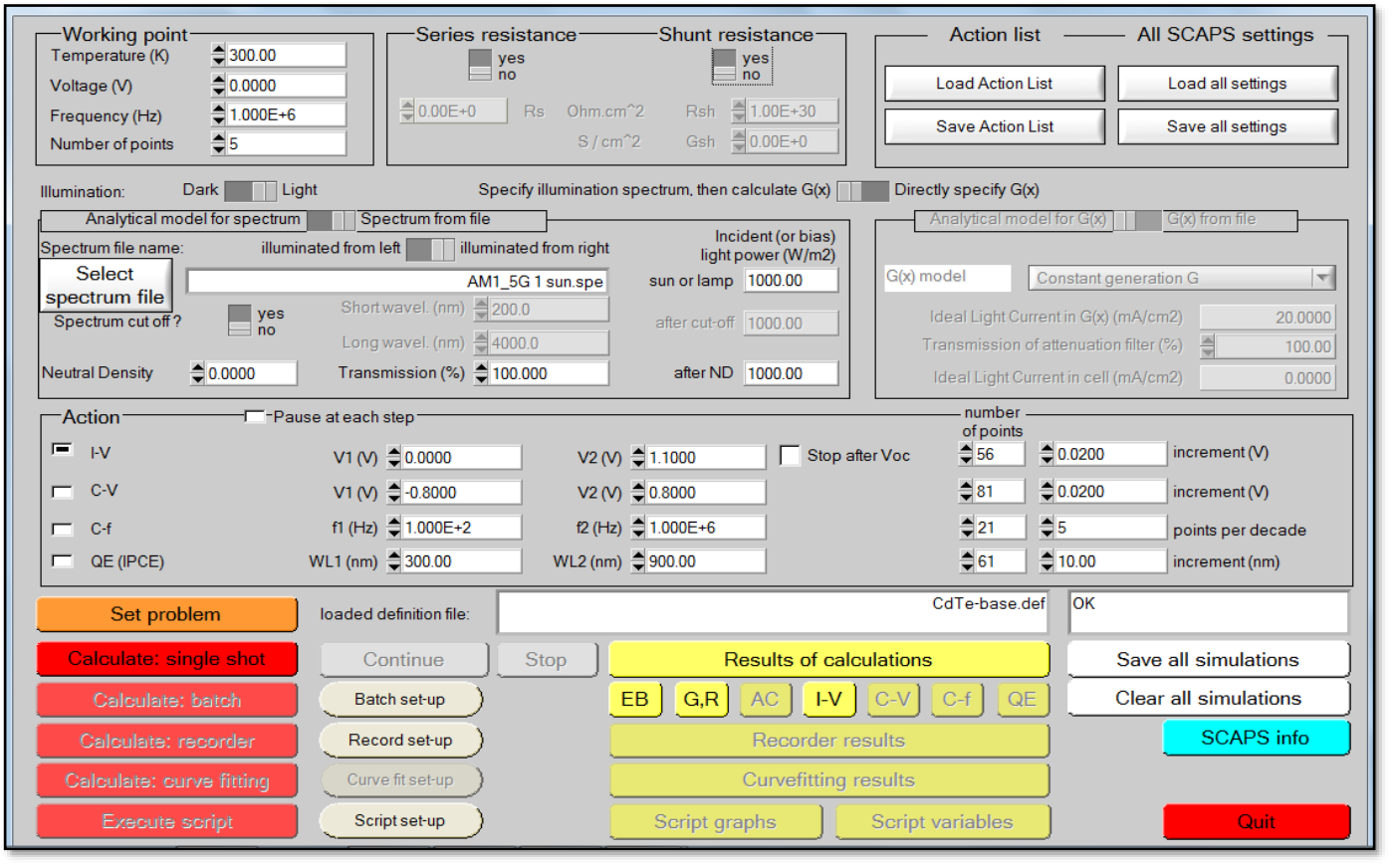

Fig. 1. SCAPS-1D action panel with all the parameters as used for the present study.

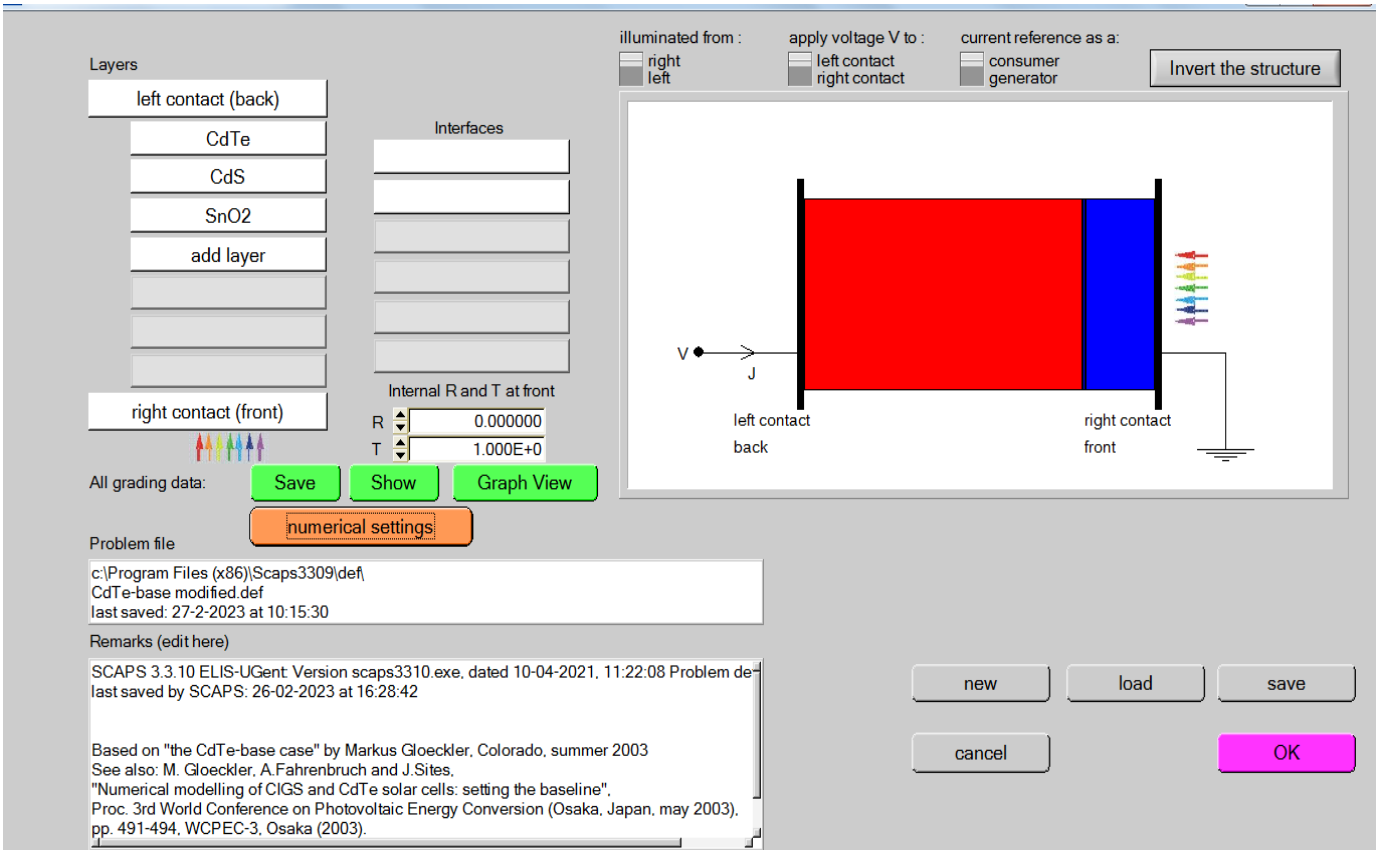

Fig. 2. Schematic illustration of SCAPS-1D panel structure based solar cell.

© Ariston Publications 2024. All rights reserved.

Table 1. Different layers parameters employed in the present simulation study.

Parameter	SnO_2	CdS	CdTe
Electron Affinity (eV)	4.0	4.0	3.9
Dielectric Permittivity (relative)	9.0	10	9.4
Electron mobility(cm^2/Vs)	100	100	320
Hole mobility(cm^2/Vs)	25	25	40
Band gap (eV)	3.6	2.4	1.5
CB density of states(cm^{-3})	2.2×10^{18}	2.2×10^{18}	8×10^{17}
VB density of states(cm^{-3})	1.8×10^{19}	1.8×10^{19}	1.8×10^{19}
Donor Density N_D(cm^{-3})	1.0×10^{19}	1.1×10^{18}	0
Acceptor Density N_A(cm^{-3})	0	0	2.0×10^{16}

Table 2. The impact of absorber thickness on solar cell parameters. At *T*=300 K, the SnO_2 layer thickness 500 nm and CdS layer thickness 25 nm respectively.

Thickness of CdTe layer (µm)	V_{OC}(V)	J_{SC}(mA/cm^2)	FF (%)	η (%)
1.0	1.0448	23.059373	88.10	21.23
1.5	1.0465	23.572951	88.12	21.74
2.0	1.0480	23.816457	88.14	22.00
2.5	1.0493	23.971897	88.15	22.17
3.0	1.0505	24.086778	88.17	22.31
3.5	1.0517	24.178259	88.18	22.42
4.0	1.0528	24.254403	88.19	22.52
4.5	1.0539	24.319595	88.19	22.60
5.0	1.0550	24.376647	88.20	22.68

3. RESULTS AND DISCUSSION

3.1. Modeling and optimization of absorber CdTe-layer thickness

The optimization of the CdTe absorber layer thickness is critical for achieving high solar cell efficiency while minimizing material usage. Table 2 presents the variation in key photovoltaic parameters—open circuit voltage (V_{OC}), short circuit current density (J_{SC}), fill factor (FF), and efficiency (η)—as the thickness of the CdTe layer increases from 1 µm to 5 µm, in increments of 0.5 µm, at a temperature of 300 K. The thicknesses of the CdS (25 nm) and SnO_2 (500 nm) layers are kept constant during the simulation to isolate the impact of the absorber layer.

As the thickness of the CdTe layer increases, the V_{OC} shows a slight but consistent increase from 1.0448 V at 1 µm to 1.0550 V at 5 µm. Similarly, the J_{SC} improves steadily due to enhanced light absorption, increasing from 23.059 mA/cm² to 24.377 mA/cm². The FF remains relatively stable, ranging between 88.10% and 88.20%, reflecting minimal losses due to resistive or recombination effects.

The most notable change is observed in the device efficiency (η), which increases progressively from 21.23% at a 1 µm thickness to 22.68% at 5 µm. This improvement highlights the importance of a thicker CdTe layer for achieving better photon absorption and charge carrier generation. However, the efficiency gains beyond a certain thickness become less significant, indicating a diminishing return on material usage.

These findings emphasize the trade-off between material consumption and efficiency optimization. While increasing the CdTe thickness enhances device performance, practical considerations such as cost and manufacturing feasibility must be addressed. For real-world applications, a balance must be struck to achieve high efficiency with minimal resource expenditure.

Figure 3 illustrates the variation in key performance parameters of the CdTe solar cell—efficiency (η%), short-circuit current density (J_{SC}), fill factor (FF%), and open-circuit voltage (V_{OC})—as a function of the absorber layer thickness, while maintaining SnO_2 and CdS layers at fixed thicknesses of 500 nm and 25 nm, respectively, at a temperature of 300 K.

One of the primary challenges in maximizing the performance of CdTe solar cells lies in determining the optimal thickness of the absorber layer. The absorber layer plays a pivotal role in the solar cell's efficiency as it is responsible for generating electron-hole pairs upon illumination. As shown in Figure 3, increasing the thickness of the CdTe layer enhances the photon absorption capacity, enabling the generation of more electron-hole pairs. This, in

 © Ariston Publications 2024. All rights reserved

turn, improves J_{SC} and, subsequently, the overall device efficiency.

The figure reveals that J_{SC} increases steadily with thickness, reflecting the ability of a thicker CdTe layer to absorb a broader spectrum of incident light. The open-circuit voltage (V_{OC}) also demonstrates a slight upward trend, attributable to improved charge carrier collection and reduced recombination losses. The fill factor (FF%) remains relatively stable, indicating consistent device performance across the range of thicknesses. The combined effect of these metrics results in a gradual increase in solar cell efficiency (η%), highlighting the importance of absorber thickness in achieving higher performance.

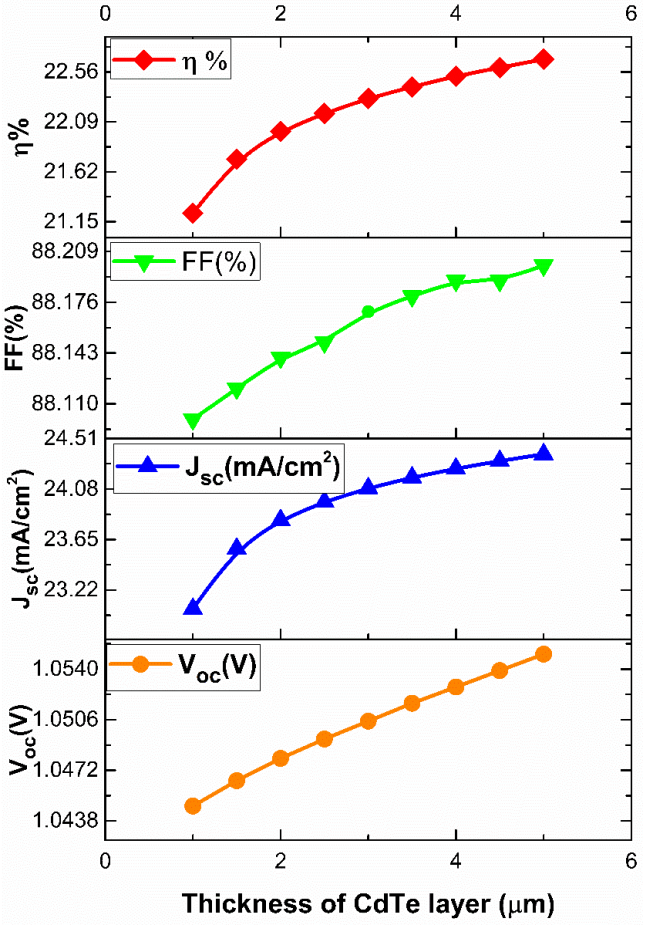

Fig. 3. The Effect of Absorber Layer Thickness on Solar Cell Efficiency Metrics: : η%, Jsc, FF%, and Voc. SnO_2 and CdS layers are 500 nm and 25 nm thick, respectively, at T=300 K.

However, practical considerations such as material costs and manufacturability must be taken into account. Excessive thickness not only increases the cost of cadmium telluride but also complicates the fabrication process, potentially leading to diminished returns on efficiency gains. Thus, while a thicker CdTe layer improves performance by absorbing more photons, optimization is necessary to balance performance with cost-effectiveness in large-scale production. The insights from Figure 3 underscore the critical need to fine-tune the absorber layer thickness to achieve both high efficiency and economic feasibility in CdTe solar cell manufacturing.

The Quantum Efficiency (QE%) of the solar cell was estimated for various CdTe thicknesses in the range of 1 to 5μm at T = 300K and is presented in Figure 4. The estimation shows that the majority of the absorption takes place in the range of 350 to 850 nm wavelength range. It is found that QE% increases with increment in of CdTe layer thickness increase up to 4 μm, significantly. The efficiency does not substantially increase layers beyond 4 microns, which indicates that this width is sufficient to absorb most of the incoming photons.

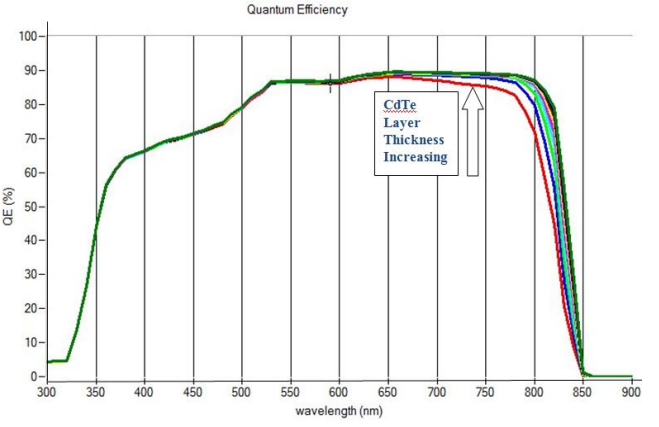

Fig. 4. The impact of thickness of CdTe layer on QE%, at T = 300K.

Since the high recombination zone at back contact and the *e-h* generation region in the cells with thinner layers are close, hence reducing the concentration of *e-h* pairs lowering QE. In contrast, the electron-hole generation process takes place far from the back of thicker CdTe layer cells [16]. J_{sc} decreases linearly below 1.5 μm CdTe layer thickness in solar cells with a thinner absorbing layer resulting in incomplete photon absorption and an increased rate of charge carrier reassembly instigated at rear contact of the cell situated close to the depletion region. The SCAPS-1D simulation results as presented in Figure 3 showed that cell efficiency increased with an increase in layer thickness CdTe absorber layer up to 4μm, and there were no discernible changes in cell efficiency for CdTe thickness was over 4μm. Therefore, the simulations show that a thickness of 4 μm with an efficiency (η) of 22.52% is ideal for the absorber CdTe layer.

3.2. Modeling and Optimization of CdS Buffer Layer Thickness

As a buffer layer, CdS has been used because of suitability of band gap at 2.4eV with CdTe [19].The goal of the study is to minimize the losses of electrical and optical nature of the radiation energy that buffer layer has induced in the incident radiation. As shown in Table 3, investigations have been done on the solar cell device performance.

© Ariston Publications 2024. All rights reserved.

Table 3. Impact of CdS layer thickness on cell efficiency parameters. At *T*=300 K, CdTe and SnO_2 layers thickness are 2 µm and 0.5 µm respectively.

Thickness of CdS layer (nm)	V_{OC}(V)	J_{SC}(mA/cm^2)	FF(%)	η (%)
35	1.0475	23.400553	88.16	21.61
30	1.0477	23.603507	88.15	21.80
25	1.0480	23.816457	88.14	22.00
20	1.0482	24.040893	88.13	22.21
15	1.0484	24.282740	88.11	22.43
10	1.0487	24.562421	88.07	22.69
07	1.0489	24.764974	88.06	22.87
06	1.0490	24.840183	88.07	22.95
05	1.0491	24.919419	88.09	23.03

At T = 300 K, efficiency as a function of CdS layer thickness ranged from 5 to 35 nm. The thickness of CdTe, SnO_2 layer to has been taken as 2 µm, 0.5 µm respectively as obtained from the literature [11-13]. The results obtained in the simulations are presented in Figure 5.

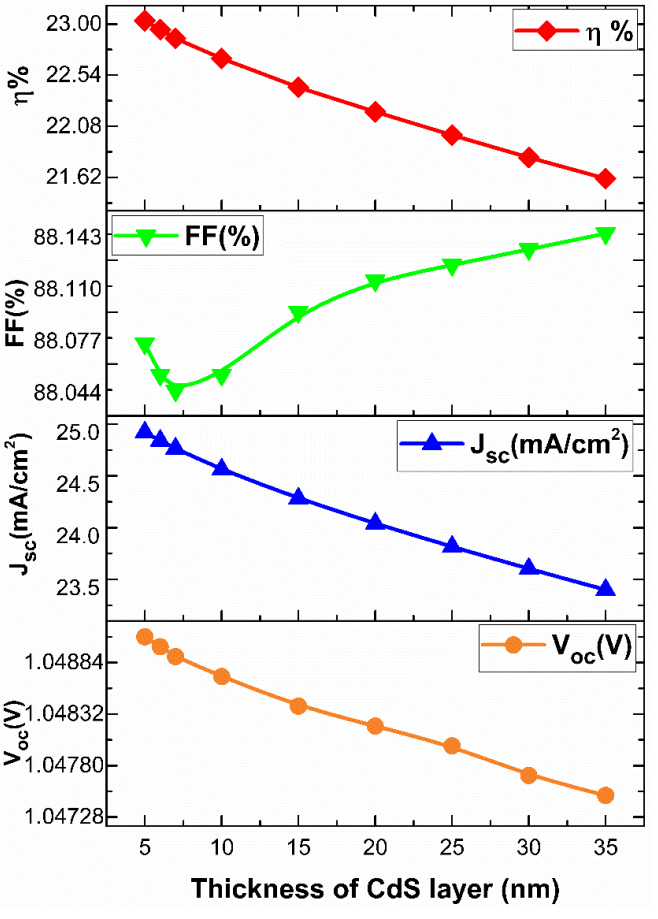

Fig. 5. The influence of the thickness of CdS layer on solar cell parameters: V_{oc}, J_{sc}, FF% and η%. At *T*=300 K, SnO_2 and CdTe layers thickness are 0.5 µm and 2 µm respectively.

It can be inferred from the figure that cell performance declines as CdS layer thickness increases from 5 nm to 35 nm. The impact on V_{OC} and FF% is not statistically significant because of large losses in a thick CdS layer. More photons from the input radiation will be absorbed by a thicker CdS layer, which will have a detrimental effect reducing the number of photons that can get through the CdTe absorber layer due to charge carrier recombination which ultimately leads to a lower QE%. It could be observed from Figure 5 that there is a significant decline in J_{sc} and η% values alongside the thickness increase of CdS films. Conversely, the CdS layer functions better and is more effective since the depletion layer is thinner. The '*lattice mismatch*' involving CdTe and CdS layer appears to cause misfit dislocation, while the decrease in depletion layer seems to counteract this effect [16]. The leakage current results from a thinner buffer layer, whereas a low carrier separation rate consequently from a thicker one. Furthermore, as the CdS thickness decreases, the quantum efficiency increases, indicating less parasitic absorption, enabling the more significant charge carrier generation in the absorber. Due to the limitations of the fabrication processes and equipment, obtaining uniform and pinhole-free CdS layers smaller than 10nm is challenging. Consequently, the optimum and desired thickness of buffer layer is taken to be 15 nm. Figure 6 indicates the impact of variation of CdS layer thickness on QE%. The findings indicate that QE% rises with the reduction of CdS layer thickness. The ratio of the number of electrons created by an incoming photon of a particular wavelength in the external circuit is known as a solar cell's quantum efficiency [20].

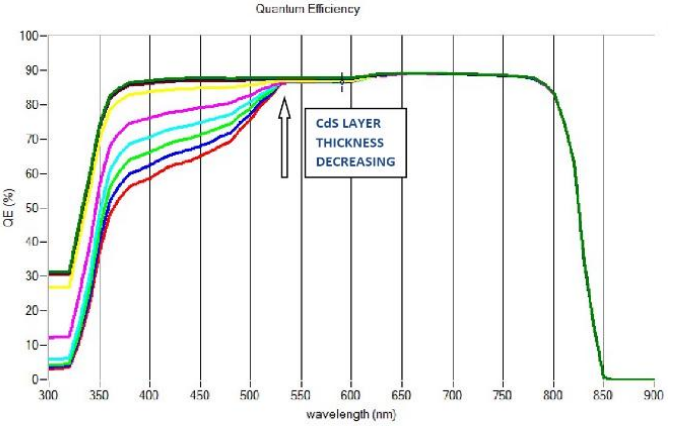

Fig. 6. The influence of CdS layer thickness on QE%, at 300K temperature.

 © Ariston Publications 2024. All rights reserved

Table 4. The impact of thickness of SnO_2 layer on cell efficiency variables. At T=300 K, CdTe and CdS layers thickness are 2000 nm and 25 nm correspondingly.

Thickness of SnO_2 layer(μm)	V_{OC}(V)	J_{SC} (mA/cm^2)	FF (%)	H (%)
0.1	1.0485	24.358791	88.13	22.51
0.2	1.0484	24.212176	88.14	22.37
0.3	1.0482	24.074236	88.14	22.24
0.4	1.0481	23.942820	88.14	22.12
0.5	1.0480	23.816457	88.14	22.00
0.6	1.0478	23.694114	88.14	21.88
0.7	1.0477	23.575060	88.14	21.77

Table 5. Solar cell parameters at 2 μm thickness of CdTe(p) layer.

Structure	EA of CdS(eV)	V_{OC}(V)	J_{SC}(mA/cm^2)	FF(%)	η (%)
CdTe(p)-CdS(n)-SnO_2(n^+)	4	0.9988	22.396291	85.34	19.09
CdTe(p)-CdS(n)-SnO_2(n^+)	4.2	0.9992	22.304253	83.61	18.63
CdTe(p)-CdS(n)-SnO_2(n^+)	3.75	0.9986	22.471254	85.74	19.24
CdTe(p^+)-CdTe(p)-CdS(n)-SnO_2(n^+)	4	1.0480	23.791211	88.07	21.96
CdTe(p^+)-CdTe(p)-CdS(n)-SnO_2(n^+)	4.2	1.0480	23.770063	87.55	21.81
CdTe(p^+)-CdTe(p)-CdS(n)-SnO_2(n^+)	3.75	1.0480	23.816457	88.14	22.00

3.3. Modeling and optimization of SnO_2 (Window) layer thickness

The perfect window layer must have sufficient conductivity to capture the charge carriers while remaining being transparent to the incident radiation [16]. SnO_2 possesses all the necessary characteristics for a window layer, including a band gap of 3.6eV (which absorbs light of 300 nm or less in the Ultra Violet C area), perfect transmission of infrared and visible radiation across the layer, and the ability to be efficiently absorbed by the CdTe layer [21]. The simulation results obtained in the present study indicates that the increase in SnO_2 layer thickness over 0.2μm hinders the device performance variables such as V_{oc}, FF%, J_{sc} and η% as summarized in Table 4. Figure 7 depicts the relationship between ITO layer thickness and device performance parameters.

3.4. Influence of Electron Affinity of CdS Layer and addition of p^+ Layer at the back

The term "*electron affinity*" of semiconductors refers to the energy difference between the bottom of the conduction band and the "vacuum level" (the minimum energy of an electron in a vacuum) whereas the "*work function*" of a semiconductor is the energy required to transfer an electron from its surface into a vacuum, estimated by the difference of vacuum level from the Fermi level. The two semiconductors' corresponding conduction band edges and valence band edges are denoted by the ΔE_c and ΔE_v, respectively [22]. In the hetero-junction device, the formation of an Ohmic or Schottky barrier depends on the electron's affinities (EA). In Table 5, the various solar cell parameters attained employing the simulations are tabulated with the variation of the electron affinity values of CdS layer and the introduction of P^+ back surface layer. Figure 8 shows due to appropriate band alignment, efficiency increases when the electron affinity is reduced [20].

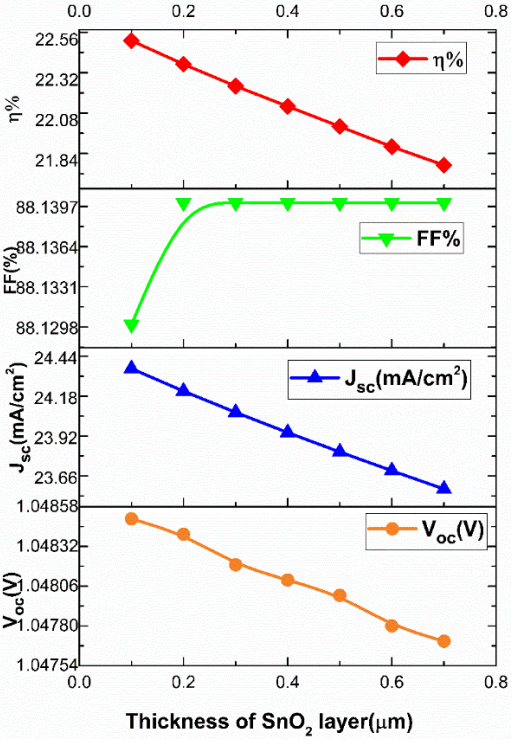

Fig. 7. The effect of SnO_2 window layer thickness variation on solar cell parameters: η%, FF%, J_{sc} and V_{oc}. The thickness CdS and CdTe layers are 25 nm and 2000 nm, respectively, at T=300 K.

© Ariston Publications 2024. All rights reserved.

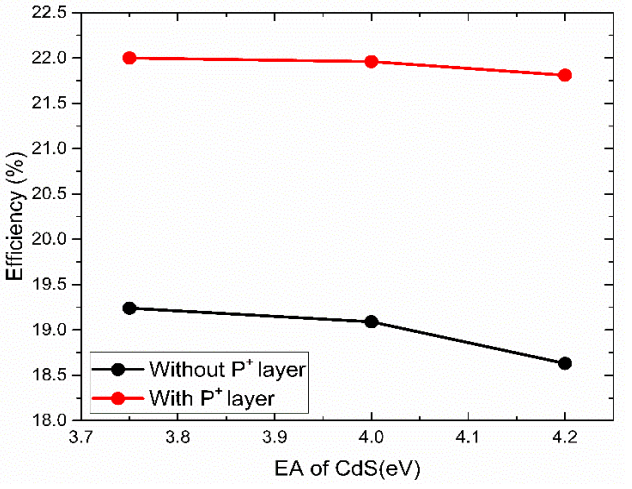

Fig. 8. Variation of efficiency with electron affinity of CdS layer for CdTe(p)-CdS(n)-$SnO_2(n^+)$ structure.

A metal back contact with a high work function is necessary to boost the cell's efficiency. Since most metals don't have high enough work functions, Schottky-barrier contact arises at the junction between the metal electrode and the absorber [23]. Due to its ability to obstruct hole transport, this Schottky barrier has a major influence on the I-V properties of a solar PV cell. Ohmic contact with the absorber layer requires a suitable metal with a high work function. Lowering the barrier height or restricting its width by severely doping an additional back surface field (BSF) P^+ layer are a few favored methods for addressing this difficulty, where P^+ layer serves as a reflector and is essential for enhancing light trapping capabilities. Enhancing back reflectivity lowers photon absorption which increases efficiency [20] which is evident from Figure 9.

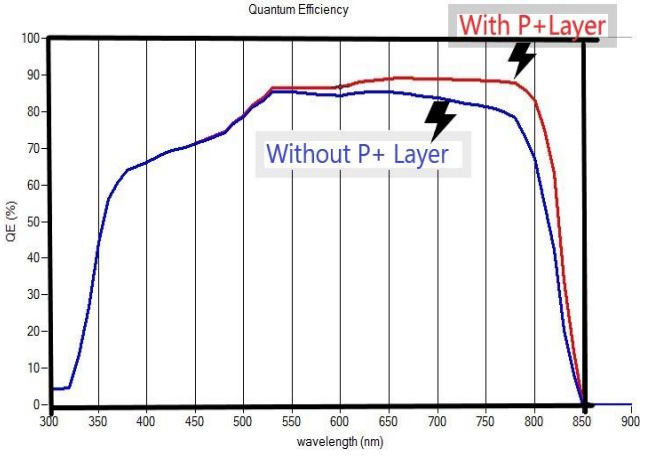

Fig. 9. Effect of adding p^+ layer to the structure CdTe(p)-CdS(n)-$SnO_2(n^+)$ on the QE% of the taken solar cell.

3.5. Current mode

Ultimately, employing input layer thickness based on optimal estimated thickness of the various layers, i.e., CdTe=4 µm, CdS=15 nm, and SnO_2=200nm at electron affinity of CdS=3.75eV, SCAPS-1D simulates the J-V curve. With previously attained optimized input parameters the highest solar cell output parameters obtained are J_{SC}=25.141mA/cm^2,V_{OC}=1.0538 V, FF%=88.16 % and η%= 23.36% which is depicted in Figure 10.

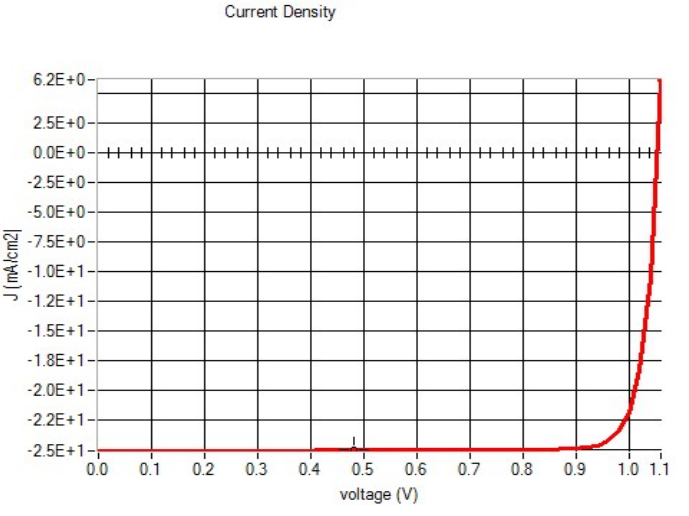

Fig. 10. J-V curve of the solar cell for optimized layer thickness at 300 K temperature.

4. CONCLUSION

The optimization of the p-type absorber layer (CdTe), an n-type buffer layer (CdS) and n^+ window layer (SnO_2) layer thicknesses, as well as the influence of the CdS layer's electron affinity and the addition of a thin, heavily doped (p+) CdTe layer as a back surface field on the PV device's performance, was studied by SCAPS-1D simulator. Simulation results revealed that the reduction of CdS electron affinity increases efficiency whereas the insertion of CdTe (p^+) as BSF considerably raises the output parameters and, consequently, enhances solar cells' efficiency. Quantum Efficiency also improves in the red region after introduction of P^+ layer. The pristine CdS/CdTe solar cell without a BSF layer has an optimized efficiency of roughly 19%. When CdTe BSF layer is added, the solar cell's efficiency increases to 23.36% with improved V_{oc} of 1.0538 V, 25.141mA/cm^2 J_{sc}, and 88.16% FF, respectively with an electron affinity 3.7eV of CdS layer.

DECLARATIONS

Ethical Approval

Not Applicable

 © Ariston Publications 2024. All rights reserved

Funding

Not applicable

Availability of data and material
The data of the manuscript are available upon request.

Conflicts of Interest

The authors declare no conflicts of interests. The authors alone are responsible for the content and writing of this article.

Authors' contributions

AR has done the simulations (with the inputs from the other authors) as well as prepared the 1st draft of the manuscript. MD, CS & AB have revised the work and edited the manuscript.

ACKNOWLEDGEMENTS

Professor Marc Burgelman and his colleagues at the University of Ghent's Department of Electronics and Information Systems deserve special recognition from the authors for creating the SCAPS software package and allowing its usage.

REFERENCES

[1] Safa Sultana, R., Bahar, A.N., Asaduzzaman, M. and Ahmed, K., **2017.** Numerical modeling of a CdS/CdTe photovoltaic cell based on ZnTe BSF layer with optimum thickness of absorber layer. *Cogent Engineering*, *4*(1), p. 1318459.

[2] Jha, P.K., Chourasia, N.K., Srivastava, A., Sharma, A.K., Kumar, R., Sharma, S., Kumar, M. and Chourasia, R.K., **2023.** Study of eco-friendly organic–inorganic heterostructure $CH_3NH_3SnI_3$ perovskite solar cell via SCAPS simulation. *Journal of Electronic Materials*, *52*(7), pp.4321-4329.

[3] Sharma, S., Jain, K.K. and Sharma, A., **2015**. Solar cells: in research and applications—a review. *Materials Sciences and Applications*, *6*(12), pp.1145-1155.

[4] Devendra, K. C., Shah, D.K., Akhtar, M.S., Park, M., Kim, C.Y., Yang, O.B. and Pant, B., **2021.** Numerical investigation of graphene as a back surface field layer on the performance of cadmium telluride solar cell. *Molecules*, *26*(11), p.3275.

[5] Green, M.A., Dunlop, E.D., Yoshita, M., Kopidakis, N., Bothe, K., Siefer, G., Hinken, D., Rauer, M., Hohl-Ebinger, J. and Hao, X., **2024.** Solar cell efficiency tables (Version 64). *Progress in Photovoltaics: Research and Applications*, *32*(7), pp.425-441.

[6] Ashraf, M., Ayaz, M., Khan, M., Adil, S.F., Farooq, W., Ullah, N. and Nawaz Tahir, M., **2023**. Recent trends in sustainable solar energy conversion technologies: mechanisms, prospects, and challenges. *Energy & Fuels*, *37*(9), pp.6283-6301.

[7] Lee, T.D. and Ebong, A.U., **2017.** A review of thin film solar cell technologies and challenges. *Renewable and Sustainable Energy Reviews*, *70*, pp.1286-1297.

[8] Scarpulla, M.A., McCandless, B., Phillips, A.B., Yan, Y., Heben, M.J., Wolden, C., Xiong, G., Metzger, W.K., Mao, D., Krasikov, D. and Sankin, I., **2023.** CdTe-based thin film photovoltaics: Recent advances, current challenges and future prospects. *Solar Energy Materials and Solar Cells*, *255*, p.112289.

[9] Correa-Baena, J.P., Saliba, M., Buonassisi, T., Grätzel, M., Abate, A., Tress, W. and Hagfeldt, A., **2017.** Promises and challenges of perovskite solar cells. *Science*, *358*(6364), pp.739-744.

[10] Mostefaoui, M., Mazari, H., Khelifi, S., Bouraiou, A. and Dabou, R., **2015.** Simulation of high efficiency CIGS solar cells with SCAPS-1D software. *Energy Procedia*, *74*, pp.736-744.

[11] Husna, J., Menon, P.S., Chelvanathan, P., Mohamed, M.A., Tripathy, S.K. and Lenka, T.R**., 2021.** Numerical study of semi-transparent thin film heterojunction p-CuO/n-ZnO/AZO/ITO solar cells device model using SCAPS-1D. *Chalcogenide Letters*, *18*(11), pp. 667-679.

[12] Di Sabatino, M., Hendawi, R. and Garcia, A.S., 2024. Silicon Solar Cells: Trends, Manufacturing Challenges, and AI Perspectives. *Crystals*, *14*(2), p.167.

[13] Rahman, M.F., Habib, M.J.A., Ali, M.H., Rubel, M.H.K., Islam, M.R., Md Ismail, A.B. and Hossain, M.K., **2022.** Design and numerical investigation of cadmium telluride (CdTe) and iron silicide ($FeSi_2$) based double absorber solar cells to enhance power conversion efficiency. *AIP Advances*, *12*(10), p. 105317.

[14] Montoya De Los Santos, I., Pérez-Orozco, A.A., Liña-Martínez, D.A., Courel, M., Meza-Avendaño, C.A., Borrego-Pérez, J.A., Pérez, L.M. and Laroze, D., **2023.** Towards a CdTe solar cell efficiency promotion: the Role of ZnO: Al and CuSCN nanolayers. *Nanomaterials*, *13*(8), p.1335.

[15] Hossain, M.K., Toki, G.I., Alam, I., Pandey, R., Samajdar, D.P., Rahman, M.F., Islam, M.R., Rubel, M.H.K., Bencherif, H., Madan, J. and Mohammed, M.K., **2023.** Numerical simulation and optimization of a $CsPbI_3$-

© Ariston Publications 2024. All rights reserved.

based perovskite solar cell to enhance the power conversion efficiency. *New Journal of Chemistry*, *47*(10), pp.4801-4817.

[16] Zyoud, S.H. and Zyoud, A.H., **2021.** Effect of absorber (acceptor) and buffer (donor) layers thickness on Mo/Cdte/Cds/ITO thin film solar cell performance: SCAPS-1D simulation aspect. *International Review on Modelling and Simulations*, *14*(1), pp.10-17.

[17] Elfarri, H., Bouachri, M., Frimane, A., Fahoume, M., Daoudi, O. and Battas, M., **2021.** Optimization of simulations of thickness layers, temperature and defect density of CIS based solar cells, with SCAPS-1D software, for photovoltaic application. *Chalcogenide Letters*, *18*(4).

[18] Burgelman, M., Nollet, P. and Degrave, S., **2000.** Modelling polycrystalline semiconductor solar cells. *Thin solid films*, *361*, pp.527-532.

[19] Ferekides, C.S., Marinskiy, D., Viswanathan, V., Tetali, B., Palekis, V., Selvaraj, P. and Morel, D.L., **2000.** High efficiency CSS CdTe solar cells. *Thin Solid Films*, *361*, pp.520-526.

[20] Barman, B. and Kalita, P.K., 2021. Influence of back surface field layer on enhancing the efficiency of CIGS solar cell. *Solar Energy*, *216*, pp.329-337.

[21] Sarah, K.E., Roland, U. and Ephraim, E.O., **2020.** A review of solar photovoltaic technologies. *International Journal of Engineering Research & Technology*, *9*(7), pp.741-749.

[22] Al Kuhaimi, S.A., **1998.** Electron affinity difference in CdS/Si solar cells. *Japanese journal of applied physics*, *37*(9R), p.4850.

[23] Sun, H.Y., Li, P.H., Xue, Y.M., Qiao, Z.X. and Sai, L.I.U., **2019.** Effect of $MoSe_2$ on the performance of CIGS solar cells. *Optoelectronics Letters*, *15*(6), pp.428-434.

 © Ariston Publications 2024. All rights reserved